Circular Superposition Spread-Spectrum Transmission for Multiple-Input Multiple-Output Underwater Acoustic Communications

Xiangzhao Qin[®], Student Member, IEEE, Fengzhong Qu[®], Senior Member, IEEE, and Yahong Rosa Zheng[®], Fellow, IEEE

Abstract—This letter proposes a circular superposition spread spectrum (CSSS) scheme for multiple input-multiple-output (MIMO) underwater acoustic (UWA) communications where the multipath channel length is long and the Doppler spread is severe. The proposed CSSS scheme divides the spreading sequence into several sub-sequences, and the circular shifting of the subsequences forms multiple spreading sequences. Each spreading sequence spreads different payload symbols individually, then the multiple spread symbols are summed to form the transmitted signal at one transducer. The CSSS signaling enables the receiver to apply a circularly shifted coherent RAKE to harvest the delay-spatial diversity of the MIMO UWA channels. If one of baseband symbol is known to the receiver, then the known symbol is utilized as the training symbol to estimate the time-variant channel impulse response (CIR) at every sub-sequence length. The receiver also reduces the co-channel interference (CCI) by exploiting the periodical auto-correlation property of the circular spreading sequences. Simulation results demonstrate that the proposed CSSS achieves more robust performance than the conventional direct sequence spread spectrum (DSSS) approach while reducing the training overhead for MIMO systems.

Index Terms—Direct-sequence spread-spectrum (DSSS), circular superposition, RAKE receiver, multiple-input multiple-output (MIMO), underwater acoustic (UWA) communications.

I. INTRODUCTION

CHIEVING reliable Underwater Acoustic (UWA) communications is recognized as a challenging problem due to the harsh doubly-selective channels: i) the channel impulse response (CIR) due to the excessive multipath delay spread induces severe intersymbol interference (ISI) across hundreds of symbol periods; ii) significant time variation and Doppler scattering impair the reliable channel tracking and coherent

Manuscript received April 21, 2019; accepted May 8, 2019. Date of publication May 16, 2019; date of current version August 12, 2019. This work of Fengzhong Qu was supported in part by the National Natural Science Foundation of China for Excellent Young Scholars under Grant 61722113, the Joint Program of National Natural Science Foundation of China and Zhejiang Province under Grant U1809211, the Open Project Program of Qingdao National Laboratory for Marine Science and Technology under Grant QNLM2016ORP0112. The work of Y. R. Zheng was supported in part by the US National Science Foundation under projects CISE-1853257 and IIP-1853258. The associate editor coordinating the review of this letter and approving it for publication was Y. Wu. (Corresponding author: Fengzhong Qu.)

X. Qin and F. Qu are with the Key Laboratory of Ocean Observation-Imaging Testbed of Zhejiang Province, Zhejiang University, Zhoushan 316021, China (e-mail: chrisqinxz@zju.edu.cn; jimqufz@zju.edu.cn).

Y. R. Zheng is with the Department of Electrical and Computer Engineering, Lehigh University, Bethlehem, PA 18015-3084 USA (e-mail: yrz218@lehigh.edu).

Digital Object Identifier 10.1109/LCOMM.2019.2917192

phase detection; iii) the limited channel bandwidth provides low frequency diversity for Orthogonal Frequency-Division Multiplexing (OFDM) or spread-spectrum schemes. [1].

Achieving high data rate and maintaining high reliability are often conflicting goals for UWA communications. To realize high data rate transmission for UWA channels, multiple-input multiple-output (MIMO) schemes have attracted much attention thanks to the temporal and spatial diversity gains, as well as multiplexing gains. Meanwhile, the processing gain provided by MIMO in the delay-spatial correlated UWA channels is limited, and MIMO co-channel interference (CCI) overwhelms the signal from a given front-end pair, especially in the fast time-varying channels. Long training pilots for channel estimation and powerful channel equalization are often required to achieve satisfactory robustness, but the more advanced the receivers are, the more computations they will consume. Therefore, it is a difficult trade-off among data rate, system performance, and complexity.

Spread-spectrum based modulation techniques have been investigated for UWA communications over the past two decades [2]–[9], including both the Direct-Sequence Spread Spectrum (DSSS) and Frequency-Hopping Spread Spectrum (FHSS). The SS schemes benefit from the low probability of detection (LPD) and low probability of interception (LPI), as well as robust receiver performance at a low received signal-to-noise ratio (SNR) [2]. By sacrificing the data rate, DSSS techniques exploit the inherent frequency diversity and the spreading gain [3]. To combat the limited bandwidth of UWA channels, differential coding metric is adopted in [4], [5] for transmission diversity. The decentralized receiver schemes, including nonlinear hypothesis feedback equalizer [6] and linear RAKE receiver [7], are investigated.

Motivated by the waveform superposition scheme in [8], this letter presents a circular superposition spread-spectrum (CSSS) transmission scheme for MIMO UWA communications. The proposed waveform exploits the ideal periodical correlation function of the chosen zero correlation zones (ZCZ) sequence [10], and enables the coherent receiver to combat the severe inter-block interference (IBI), the CCI from the inner superimposed symbols, and the multiplexing access interference (MAI) from multiple transmit front-end pairs. Simulation results demonstrate the effectiveness of the proposed scheme in fast time-varying and frequency-selective UWA channels.

Notation: Upper (lower) boldface letters are used for matrices (column vectors). $(\cdot)^H$, $(\cdot)^T$ and $(\cdot)^*$ repre-

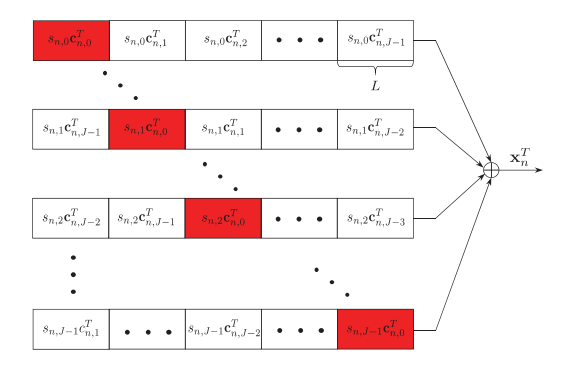


Fig. 1. Structure of the baseband waveform at the nth transducer.

sent the Hermitian, transpose, and conjugation, respectively. In addition, I denotes the identity matrix, $\|\cdot\|^2$ is the squared Frobenius norm of a vector or matrix, $|\cdot|$ is the scalar norm, and $|\cdot|$ denotes the floor function. The $i \times j$ complex matrix space is represented by $C^{i \times j}$. Other mathematical symbols are defined after their initial appearance.

II. SYSTEM MODEL

Consider an $N \times M$ MIMO communication system, where N and M are the numbers of the transducers and receivers, respectively. Each transducer adopts one K-length unimodular spreading sequence $\{\mathbf{c}_n = [c_{n,0},\ldots,c_{n,K-1}]^T\}_{n=1}^N$ to spread J payload symbols $s_{n,j}$ for $j = 0, \ldots, J-1$. For the traditional DSSS system, payload symbol $s_{n,j}$ is spread by a unique spreading sequence, and the baseband waveform of the nth transducer is

$$\mathbf{x}_{n,j} = s_{n,j} \mathbf{c}_n,\tag{1}$$

The transmitted baseband waveform \mathbf{x}_n is then concatenated by $\mathbf{x}_n = [\mathbf{x}_0^T, \mathbf{x}_{n,1}^T, \dots, \mathbf{x}_{n,J-1}^T]^T$. In contrast, the proposed CSSS scheme divides the

K-length spreading sequence \mathbf{c}_n into J sub-sequences $\mathbf{c}_{n,j} =$ $[c_{n,jL}, c_{n,jL+1}, \cdots, c_{n,(j+1)L-1}]^T$ for $j = 0, 1, \cdots, J-1$, where L is the maximum channel length. The circular shifting of \mathbf{c}_n by (iL) chips gives

$$\tilde{\mathbf{c}}_{n,j} = \left[\mathbf{c}_{n,J-j}^T, \dots, \mathbf{c}_{n,j}^T, \dots, \mathbf{c}_{n,J-j-1}^T \right]^T \\
= \left[c_{n,K-jL}, \dots, c_{n,K-1}, c_{n,0}, \dots, c_{n,K-jL-1} \right]^T \\
= \left[c_{n,j,0}, c_{n,j,1}, \dots, c_{n,j,K-1} \right]^T.$$
(2)

The CSSS then spreads the J symbols with the phaseshifted spreading sequences $\tilde{\mathbf{c}}_{n,j}$ and sum them together as

$$\mathbf{x}_{n} = \sum_{j=0}^{J-1} s_{n,j} \tilde{\mathbf{c}}_{n,j} = [\mathbf{x}_{n,0}^{T}, \mathbf{x}_{n,1}^{T}, \dots, \mathbf{x}_{n,J-1}^{T}]^{T}$$
(3)

Figure 1 illustrates the baseband structure of the nth transducer corresponding to (3). The maximum length J of the superimposed symbols is selected such that $J \leq \lfloor \frac{K}{L} \rfloor$, which prevents the auto-correlation property of the circular spreading sequences $\tilde{\mathbf{c}}_{n,j}$ from being impaired by the multipath UWA

After cyclic prefix (CP) insertion at the transmitter and CP removal at the receiver on a block-by-block basis, the equivalent baseband input and output (I/O) relationship is given by

$$y_{m,k} = \sum_{n=1}^{N} \sum_{l=0}^{L-1} h_{m,n}(k,l) x_{n,k-l} + w_{m,k}$$

$$= \sum_{n=1}^{N} \sum_{l=0}^{L-1} \sum_{j=0}^{J-1} h_{m,n}(k,l) s_{n,j} c_{n,j,k-l} + w_{m,k}, \quad (4)$$

where $\{h_{m,n}(k,l)\}_{l=0}^{L-1}$ is the lth channel tap between the nth transducer and the mth hydrophone at time instant kover the period of the superimposed vector \mathbf{x}_n , and $w_{m,k}$ is the additive white Gaussian noise (AWGN) with variance σ^2 . When the time duration of the baseband waveform $\{x_{n,k}\}_{k=0}^{K-1}$ is less than the channel coherence time, the channel tap is approximated as time-invariant, i.e., $h_{m,n}(k,l) \approx h_{m,n}(l)$. The system model is then rewritten as

$$\mathbf{y}_m = \sum_{n=1}^{N} \sum_{j=0}^{J-1} s_{n,j} \mathbf{C}_{n,j} \mathbf{h}_{m,n} + \mathbf{w}_m,$$
 (5)

where

$$\mathbf{y}_{m} = [y_{m,0}, \dots, y_{m,K-1}]^{T} \in \mathcal{C}^{K \times 1}$$

$$\mathbf{h}_{m,n} = [h_{m,n}(0), \dots, h_{m,n}(L-1)]^{T} \in \mathcal{C}^{L \times 1}$$

$$\mathbf{w}_{m} = [w_{m,0}, \dots, w_{m,K-1}]^{T} \in \mathcal{C}^{K \times 1}$$

The AWGN vector \mathbf{w}_m is assumed to be circularly symmetric independent and identically distributed (i.i.d) denoted as $\mathcal{CN}(\mathbf{0}, \sigma^2 \mathbf{I})$. The matrix $\mathbf{C}_{n,j}$ is defined as

$$\mathbf{C}_{n,j} = \begin{bmatrix} c_{n,j,0} & c_{n,j,K-1} & \cdots & c_{n,j,K-L+1} \\ c_{n,j,1} & c_{n,j,0} & \cdots & c_{n,j,K-L+2} \\ \vdots & \vdots & \ddots & \vdots \\ c_{n,j,K-1} & c_{n,j,K-2} & \cdots & c_{n,j,K-L} \end{bmatrix} .$$
 (6)

Equation (6) makes sense by exploiting the CP operation, and $\mathbf{C}_{n,j}$ becomes an equivalent circulant matrix.

III. RECEIVER DESIGN

The circularly shifted coherent RAKE receiver exploits the periodical auto-correlation of the spreading sequences to eliminate the CCI from the inter superimposed baseband waveform and the MAI from other front-end pairs. We assess the impact of the auto-correlation on the output of each RAKE finger. Figure 2 shows the structure of the proposed circularly shifted MIMO RAKE receiver.

The received baseband signal \mathbf{y}_m is first projected onto the local de-spreading vector $\tilde{\mathbf{c}}_{n,j}^{(l)}$ which is the circular shift version of the spreading sequence $\tilde{\mathbf{c}}_{n,j}$ by l chips with lcorresponding to the lth channel tap. The output of each RAKE finger, denoted $d_{m,n,j}^{(l)}$, is weighed by the channel coefficient $h_{m,n}(l)$, and then the outputs of L fingers are summed to yield branch output $\hat{s}_{m,n,j}$. The M branches corresponding to the received signals $\{\mathbf{y}_m\}_{\substack{m=0\\m \geq 1}}^{M-1}$ are summed and decision is made for each symbol $\{\hat{s}_{n,j}\}_{\substack{n=1,j=0\\m \geq 1}}^{N,J-1}$. Since the vector $\tilde{\mathbf{c}}_{n,j}^{(l)}$ is the (l+1)th column of $\mathbf{C}_{n,j}$ as

$$\tilde{\mathbf{c}}_{n,j}^{(l)} = [c_{n,j,K-l}, \dots, c_{n,j,0}, c_{n,j,1}, \dots, c_{n,j,K-l-1}]^T, \quad (7)$$

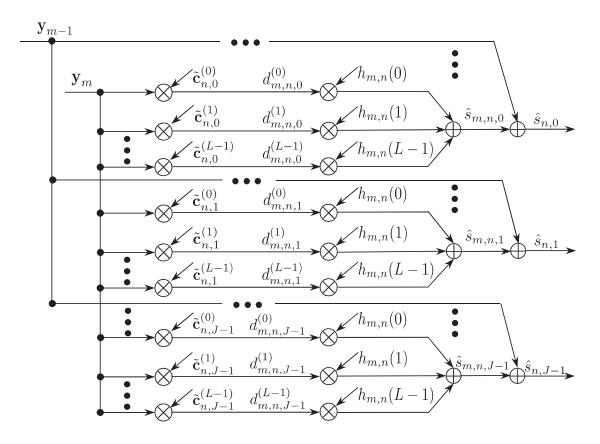


Fig. 2. Structure of the circularly shifted coherent RAKE receiver corresponding to the *n*th transducer.

for $l = 0, \dots, L - 1$, the projection output is expressed as

$$\tilde{\mathbf{c}}_{n,j}^{(l)H}\mathbf{C}_{n,j} = [r_{n,j,K-l}, \dots, r_{n,j,0}, \dots, r_{n,j,K-l-1}], \quad (8)$$

where the auto- and cross-correlation functions of $\{c_{n,j,k}\}_{k=0}^{K-1}$ is [11]

$$r_{n,j,0} = \sum_{k=0}^{K-1} c_{n,j,k} c_{n,j,k}^* = K$$

$$r_{n,j,i} = \sum_{k=0}^{K-i-1} c_{n,j,k} c_{n,j,k+i}^* + \sum_{k=K-i}^{K-1} c_{n,j,k} c_{n,j,k+i-K}^*,$$
for $i = 1, 2, \dots, K-1$. (9)

Note $r_{n,j,0} = K$ holds because the spreading sequence is of uni-modular. The output of a RAKE finger $d_{m,n,j}^{(l)}$ is then

$$d_{m,n,j}^{(l)} = \tilde{\mathbf{c}}_{n,j}^{(l)H} \sum_{n=1}^{N} \sum_{j=0}^{J-1} s_{n,j} \mathbf{C}_{n,j} \mathbf{h}_{m,n} + \tilde{\mathbf{c}}_{n,j}^{(l)H} \mathbf{w}_{m}$$

$$= s_{n,j} r_{n,j,0} h_{m,n}(l) + \tilde{\mathbf{c}}_{n,j}^{(l)H} \sum_{n'=1}^{N} \sum_{j'=0}^{J-1} s_{n',j'} \mathbf{C}_{n',j'} \mathbf{h}_{m,n}$$

$$+ w_{n,j}^{(l)}, \quad n' \neq n \text{ or } j' \neq j,$$
(11)

where $\{w_{n,j}^{(l)}\}_{l=0}^{L-1} \sim \mathcal{CN}(0,r_{n,j,0}\sigma^2)$ is complex Gaussian noise. The second term in (11) are the CCI and MAI to be eliminated. Ideally, we would like to have

$$r_{n,i,i} = 0, \quad i \in [1, L-1] \cup [K-L+1, K-1], \quad (12)$$

when K>2L-1 so that the second term in (11) vanishes. Luckily, the ZCZ sequence has been shown [10] to have "half-zone" perfect auto-correlation, i.e., $r_{n,j,i}=0,\ i\in[1,K/4-1]\cup[K/4+1,K-1]$. Therefore, we set the superimposition length to the maximum channel length and let $L\leq K/4$ to achieve interference free since

$$\tilde{\mathbf{c}}_{n,j}^{(l)H} \sum_{n'=1}^{N} \sum_{j'=0}^{J-1} s_{n',j'} \mathbf{C}_{n',j'} \mathbf{h}_{m,n} = 0, \quad n' \neq n, \text{ or } j' \neq j.$$
(13)

The RAKE outputs $\{d_{m,n,j}^{(l)}\}_{l=0}^{L-1}$ over the M hydrophones are weighted by the estimated channel taps $\hat{h}_{m,n}(l)$ with

TABLE I SIMULATION PARAMETER SETUP

Carrier Frequency	$f_c = 13 \text{ kHz}$
Sampling Rate	$f_s = 39.06 \text{ kHz}$
Bandwidth	$f_B = 7.8125 \text{ kHz}$
Number of Transducers	N = 2
Sequence Length	K = 1024
CP Length	$N_{\rm cp} = 101$
Channel Length	L = 100
Modulation Size	QPSK, 8PSK, 16QAM
Number of Superimposed Symbols	J = 5

quantitative signal-to-noise ratio (SNR). By collecting the delay-spatial diversity, the transmitted symbol is then estimated by summing the M branches:

$$\hat{s}_{n,j} = \frac{\sum_{m=1}^{M} \sum_{l=0}^{L-1} d_{m,n,j}^{(l)} \hat{h}_{m,n}^{*}(l)}{r_{n,j,0} \sum_{m=1}^{M} \sum_{l=0}^{L-1} \left| \hat{h}_{m,n}(l) \right|^{2}}$$

$$= s_{n,j} + \frac{\sum_{m=1}^{M} \sum_{l=0}^{L-1} w_{n,j}^{(l)} \hat{h}_{m,n}^{*}(l)}{K \sum_{m=1}^{M} \left\| \hat{\mathbf{h}}_{m,n} \right\|^{2}}, \tag{14}$$

where the second term in (14) contains the estimation error which is related to the noise, i.e., the larger the spreading sequence length K, the smaller the RAKE receiver error.

Note here we ignore the error between the true channel taps $h_{m,n}(l)$ and the estimated channel $\hat{h}_{m,n}(l)$. Assuming that the channel is time-invariant within the sequence block and the equivalent channel is on the "chip" level, this letter adopts $\{s_{n,0}\}_{n=1}^{N}$ as the training symbols to estimate the channel by

$$\hat{h}_{m,n}(l) = \frac{d_{m,n,0}^{(l)}}{K s_{n,0}}, \quad l = 0, \dots, L - 1, \tag{15}$$

This is straightforward from (11).

IV. SIMULATION AND RESULTS

The proposed CSSS approach was tested under the realistic sea trial MIMO UWA channels. The simulation adopts the direct-replay method in [12]. The chosen spreading sequence is zero correlation zones (ZCZ) sequence. The detailed parameter setup is illustrated in Table I.

The simulated channel is truncated from undersea 2008 Surface Processes and Acoustic Communications Experiment (SPACE08) where the the communication distance was 200 m at a sea depth of 15 m. A 4-transducer vertical array was deployed with the top transducer in the array approximately three meters above the bottom, and a 16-hydrophone vertical array was adopted with the top of array 3.25 meters above the sea floor. The carry frequency, sampling rate and bandwidth were consistent with the simulation environment. The down sampling baseband CIR distribution and equivalent channel coherence time are depicted in Fig. 3. The CIRs are timevariant (first sub-figure), in which the coherence time are used to evaluate the correlation level. The coherence level decreased to 0.4 at 0.125 s, spanning $0.125 \times 7.1825 \approx 1000$

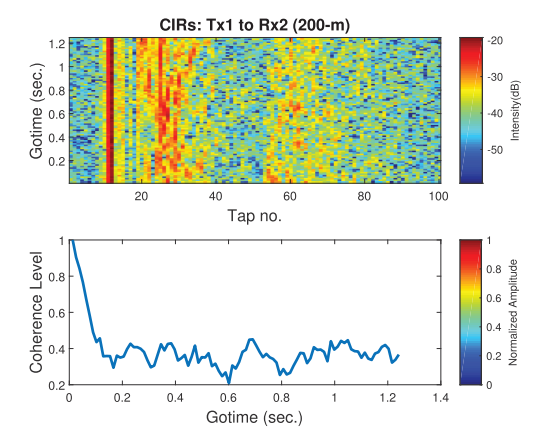


Fig. 3. The underwater channel CIR and its coherence time: from Transducer 1 to Hydrophone 2 at 200 m range.

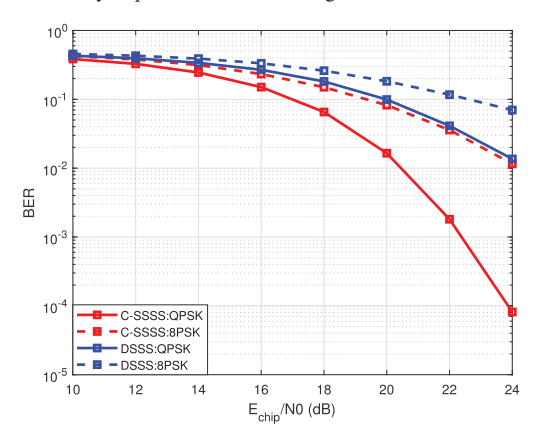


Fig. 4. BER comparison of CSSS and conventional DSSS, two transducers and four hydrophones.

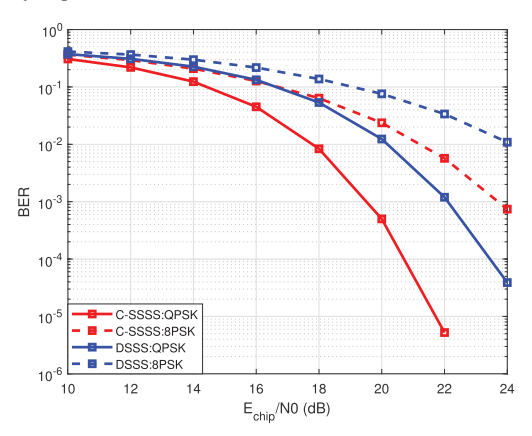


Fig. 5. BER comparison of CSSS and conventional DSSS, two transducers and eight hydrophones.

spreading chips. The CIRs were changing upon each instant k when the signals were convoluted with the UWA channels.

Two configurations were used to test the performance of the proposed CSSS scheme in comparison to the traditional DSSS. The number of the transducers was two for both configurations, and the numbers of the hydrophones were four and eight, respectively. To make a fair comparison, the DSSS counterpart also shares the same data rate by carrying the same symbols in (1) and the same CP length. Besides, all the other simulation setup remains consistent with the proposed CSSS scheme. The BER curves of the proposed CSSS and the conventional DSSS are depicted in Fig. 4 and Fig. 5.

For the CSSS approach itself, the QPSK modulation outperforms the 8PSK by 4 dB of the chip-to-noise ratio (CNR), at the BER of 10^{-2} . Moreover, the simulation result demonstrates two order of magnitude improvement of BER performance over the conventional DSSS scheme at 24 dB of CNR. The BER performance with higher 8PSK degraded due to the lower unit chip energy and the channel estimation accuracy at lower CNR. Nevertheless, the proposed CSSS method with higher order modulation still outperforms the conventional DSSS. More processing gain is observed in the eight-hydrophone configuration. For QPSK modulation, the eight-hydrophone configuration outperforms the four-hydrophone configuration by 3 dB at BER = 10^{-3} .

V. CONCLUSION

This letter proposes a robust CSSS scheme for MIMO UWA communications. By exploiting the periodical sequence superposition and CP operation, all the superimposed sequences modulate multiple symbols simultaneously and experience the same channel state, releasing the influence of channel variation on the waveform sequence. The improved RAKE receiver takes advantage of the perfect correlation property of the spreading sequence, the target front-end sequence can be detected out of the CCI and MAI. Simulation results demonstrate that the proposed CSSS outperforms the conventional DSSS under the time-varying UWA channels.

REFERENCES

- D. B. Kilfoyle and A. B. Baggeroer, "The state of the art in underwater acoustic telemetry," *IEEE J. Ocean. Eng.*, vol. 25, no. 1, pp. 4–27, Jan. 2000.
- [2] T. C. Yang and W.-B. Yang, "Low probability of detection underwater acoustic communications using direct-sequence spread spectrum," J. Acoust. Soc. Amer., vol. 124, no. 6, pp. 3632–3647, Sep. 2008.
- [3] T. C. Yang and W. B. Yang, "Performance analysis of direct-sequence spread-spectrum underwater acoustic communications with low signalto-noise-ratio input signals," *J. Acoust. Soc. Amer.*, vol. 123, no. 2, pp. 842–855, Feb. 2008.
- [4] T. C. Yang and W.-B. Yang, "Interference suppression for code-division multiple-access communications in an underwater acoustic channel," *J. Acoust. Soc. Amer.*, vol. 126, no. 1, pp. 220–228, Jul. 2009.
- [5] Z. Liu, K. Yoo, T. C. Yang, S. E. Cho, H. C. Song, and D. E. Ensberg, "Long-range double-differentially coded spread-spectrum acoustic communications with a towed array," *IEEE J. Ocean. Eng.*, vol. 39, no. 3, pp. 482–490, Jul. 2014.
- [6] M. Stojanovic and L. Freitag, "Multichannel detection for wideband underwater acoustic CDMA communications," *IEEE J. Ocean. Eng.*, vol. 31, no. 3, pp. 685–695, Jul. 2006.
- [7] J. Ling, H. He, J. Li, W. Roberts, and P. Stoica, "Covert underwater acoustic communications," *J. Acoust. Soc. Amer.*, vol. 128, no. 5, pp. 2898–2909, 2010.
- [8] F. Qu, L. Yang, and T. C. Yang, "High reliability direct-sequence spread spectrum for underwater acoustic communications," in *Proc. OCEANS*, Biloxi, MS, USA, Oct. 2009, pp. 1–6.
- [9] F. Qu, X. Qin, L. Yang, and T. C. Yang, "Spread-spectrum method using multiple sequences for underwater acoustic communications," *IEEE J. Ocean. Eng.*, vol. 43, no. 4, pp. 1215–1226, Oct. 2018.
- [10] P. Z. Fan, N. Suehiro, N. Kuroyanagi, and X. M. Deng, "Class of binary sequences with zero correlation zone," *Electron. Lett.*, vol. 35, no. 10, pp. 777–779, May 1999.
- [11] D. Chu, "Polyphase codes with good periodic correlation properties (Corresp.)," *IEEE Trans. Inf. Theory*, vol. IT-18, no. 4, pp. 531–532, Jul. 1972.
- [12] R. Otnes, P. A. van Walree, and T. Jenserud, "Validation of replay-based underwater acoustic communication channel simulation," *IEEE J. Ocean. Eng.*, vol. 38, no. 4, pp. 689–700, Oct. 2013.